Journal of Coastal Research	SI 50	432 - 437	ICS2007 (Proceedings)	Australia	ISSN 0749.0208

Waves and Climate Change on the Australian Coast

M.A. Hemer†, J.A. Church†‡ and J.R. Hunter‡

†CSIRO Marine and Atmospheric Research
Hobart, TAS 7001 Australia
mark.hemer@csiro.au
john.church@csiro.au

‡ Antarctic Climate and Ecosystems
Co-operative Research Centre.
University of Tasmania. Hobart
TAS 7001 Australia
john.hunter@utas.edu.au

ABSTRACT

HEMER, M.A.; CHURCH, J.A. and HUNTER, J.R., 2007. Waves and climate change on the Australian coast, SI 50 (Proceedings of the 9th International Coastal Symposium), 432 – 437. Gold Coast, Australia, ISSN 0749.0208.

There is a need to plan for the impacts of coastal erosion in response to climate change Australia-wide. A deep-water wave climatology of the Australian region is determined, which is required as boundary conditions for coastal wave models. Available wave data for the Australian region has been analysed to determine the mean climatology and interannual variability of mean significant wave height. Available data includes global wave model output from the ECMWF 45-yr re-analysis, ERA-40; corrected ERA-40 wave heights and the NOAA WaveWatch III operational wave model; satellite altimetry measurements; and data from a network of 30 wave-rider buoys surrounding the Australian coast located on the inner-mid continental shelf and some short-term deep-water wave-rider buoy deployments. These data have been analysed to determine the long-term mean, annual cycle and interannual variability of the mean Australian wave climate. Correlation with a number of climate indices in the Australian region indicate that southern ocean wind anomalies are a dominant mechanism responsible for variability of wave climate in the region. Correlation between monthly mean significant wave heights and the Southern Oscillation Index is significant along Australia's eastern margin.

ADDITIONAL INDEX WORDS: *Climatology, waves, Australia*

INTRODUCTION

Coastal zones are experiencing rapid development both within Australia and Internationally (AGO, 2006). As sea-level rises, the threat of coastal erosion has become an increasing and real concern. The effects of sea-level rise will be observed most severely in response to the magnitude and frequency of storm-driven (wave and storm surge) events, resulting in wave-induced erosion of coastal landforms. Climate change research priorities for the coastal environment should therefore consider changes to the wind and wave climates, as well as sea-level rise.

Climate variability and change has a significant impact on wind and wave conditions. Studies have shown that over a large area of the North Atlantic and Norwegian Sea, wave heights have increased over the last few decades with inter-annual variability as great as 20 % (WOOLF *et al*., 2002). This and similar variations in wave climate in the Mediterranean Sea (LIONELLO and SANNA, 2005) have been shown to correlate strongly with the 'North Atlantic Oscillation'. Studies of the New Zealand wave climate display a strong correlation with El-Nino events (LAING, 2000).

In the Australian region, wave-climate studies have concentrated on specific locations derived from individual buoy records, predominantly focussed on the East Coast (e.g., SHORT and TRENEMAN, 1992, ALLEN and CALLAGHAN, 2000, KULMAR, 2000, GOODWIN, 2005). With the combined advent of rapid coastal development and increasing risk due to climate change, coastal councils Australia-wide are beginning to plan for coastal erosion in response to climate change (WALSH *et al*., 2004). Therefore, a wave climatology for the entire Australia region is required, from which estimates of the wave component of coastal sea level may be determined.

This manuscript is presented in four sections. The data available for describing the Australian wave climate is presented in the next section. This is followed by an assessment of the accuracy of each of these datasets against available waverider buoy data in the Australian region and a description of the mean and annual cycle of significant wave heights (H_S) for the entire Australian region. Finally, interannual variability of the wave climate is considered by assessing correlation to a number of climate indices. This information is a critical starting point from which we will determine the variability and trends of the wave climate in the Australian region.

AVAILABLE DATA

Several wave data sets are available in the Australian region. Those considered in this research are outlined here. Figure 1 summarises the available data by total data-count per year.

The European Centre for Medium-Range Weather Forecasts (ECMWF) carried out a re-analysis of global meteorological variables, ERA-40. The period of the re-analysis is from September, 1957 to August, 2002 (45 years) and includes ocean surface wind waves on a 1.5° x 1.5° latitude-longitude grid covering the whole globe, generated using ECMWF's coupled WAM wave model (KOMEN *et al*., 1994). A subset of the re-analysis output, including H_S, mean wave period and mean wave direction, on a 2.5° x 2.5° latitude-longitude grid at 6-hourly intervals, is available from ECMWF (ECMWF, 2006).

CAIRES & STERL (2005) observed disagreement between ERA-40 modelled and observed H_S. They used a non-parametric correction to create a new 45-year global six-hourly dataset (the C-ERA-40 dataset) which improved model-to-observation comparisons. The C-ERA-40 dataset was made available at 1.5° x 1.5° latitude-longitude resolution of the original ECMWF model grid for the same period as the ERA-40 data.

The NOAA WaveWatch III (NWW3) model is a global implementation of the WAVEWATCH III 3rd generation spectral wave model (TOLMAN, 1999) developed at NOAA/NCEP. The NWW3 model has been run operationally on a 1° x 1.25° latitude-longitude grid since the beginning of 1997; and H_S; peak wave period and peak wave direction have been archived at 3-hourly intervals since the model's commencement. Archived NWW3 data have been obtained for the Australian region for the period February, 1997 to January, 2006.

Wave-rider buoy data was obtained from five organisations that operate a total of 27 wave-rider buoys in the Australian region. The first operational waverider buoy to be deployed in the Australian region was the Port Kembla, NSW buoy deployed in 1974. The network has been continuously added to, with the most recent addition being the Esperance (WA) deployment in 2006. Multi-year waverider buoy data for non-operational deployments is available from a further three sites.

Satellite altimeters measure the wave height from the shape of radar return pulse. Each altimeter mission, including GEOSAT, ERS-1, ERS-2, TOPEX, JASON-1, ENVISAT and GFO has collected global measurements of H_S at various spatial and temporal resolutions. Altimeter data were downloaded from the TUDelft RADS database (SCHRAMA *et al*, 2000). The total altimeter dataset spans a period from 1985 to present.

INTERCOMPARISON OF AUSTRALIAN WAVE DATA

Data from each source were compared with the waverider buoy data. The buoy data were chosen as the principal data, as these data were considered to have greatest accuracy.

ERA-40 Re-analysis Global Wave Model

The Australian wave-rider buoys are mid-inner-shelf buoys. The resolution of the ERA-40 wave data (2.5° x 2.5°) is not able to resolve the location of several waverider buoys that occur in land grid points. ERA-40 wave model H_S were therefore taken from the nearest wet grid point to the waverider buoy. No spatial interpolation between grid points was carried out, as buoys were located on the land side of grid cell centres. Similarly, no time interpolation was carried out. ERA-40 wave heights were related to buoy-measured wave heights by choosing the nearest H_S value in time to a buoy observation. If the time error were greater than three hours (i.e., there was no ERA-40 modelled H_S), the buoy observation was ignored. Therefore, significant geophysical variance is present between buoy and ERA-40 H_S values that remain unquantified. For the 30 buoys from which data were available, a total of 340494 corresponding H_S values was obtained. Of the 30 buoys, only 16 are expected to produce realistic estimates. For example, locations such as the Port of Melbourne waverider buoy off Point Nepean is not expected to produce reasonable comparison as Bass Strait is unresolved by the model resolution. For the 16 remaining buoys, 207124 corresponding buoy-ERA-40 H_S values were obtained. Scatter plots, regression statistics and bias were determined for each buoy independently (not shown), and for all data combined (Figure 2A). The regression slope being less than 1 (0.716), and positive intercept (0.7697) indicates small waves are overestimated, and large waves are underestimated, consistent with ERA-40 to NDBC-NOAA buoy comparisons (CAIRES and STERL, 2005).

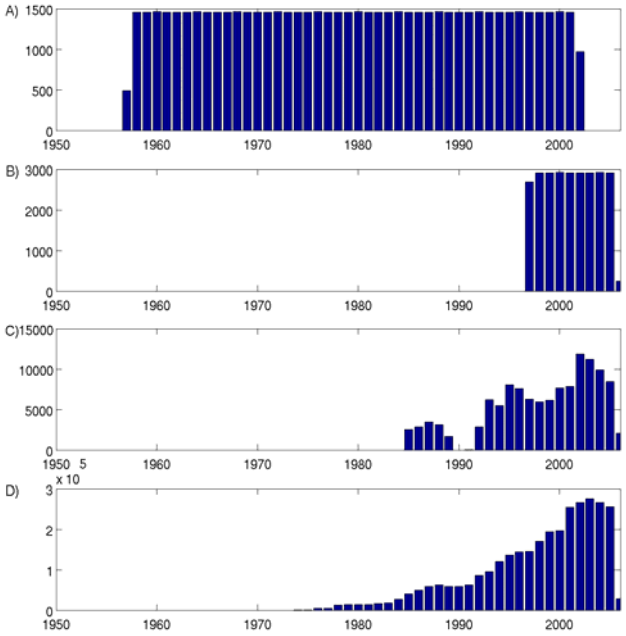

Figure 1. Summary of data available for the study. a) ERA-40 and C-ERA-40 count of data per grid cell per year; b) NWW3 count of data per grid cell per year; c) Altimeter missions, count of wave observations per 2° grid cell; d) Waverider buoy data, total number of observations per year

C-ERA-40 wave data

The corrected ERA-40 (C-ERA-40) wave dataset produced by CAIRES and STERL (2005) is available at a slightly greater resolution than the ERA-40 data; however, the resolution remains insufficient to resolve many of the buoy locations. The same approach to align model and buoy wave height data was taken (nearest grid cell to buoy, nearest time with time error less than three hours) as defined for the ERA-40 data. Including all 30 buoys, 368879 data points were aligned. Again, this was reduced to the 16 buoys located on well-resolved coastlines, reducing the number of aligned H_S values (N) to 259843. In relation the regression statistics obtained from the ERA-40 comparison, the increased slope (0.869), and reduced intercept (0.4505) values indicate that the C-ERA-40 model output improves buoy-model H_S comparisons (Figure 2B).

NWW3 Wave Model

The NOAA WAVEWATCH III (NWW3) model has a higher resolution model grid than ERA-40 allowing additional buoys to be resolved in the model coastline. The temporal resolution of the NWW3 output (three hours) reduces the geophysical variance. The same approach of choosing model output from the nearest grid-cell to the buoy and data nearest in time was used. Co-aligned H_S values from all 30 buoys total 440849 points. 313762 points are taken from the 16 'exposed' buoys. The regression slope (0.955) indicates that the NWW3 model reproduces large wave events with greater ability than the ERA-40 datasets (corrected or otherwise). The large intercept (0.4784) indicates the bias is similar to the ERA-40 data (Figure 2C).

Altimeter-measured wave heights

Significant wave heights were obtained from seven altimeter missions. Previous studies of wave height measurements from altimeters indicate these data require correction to generate consistent and homogeneous data. Several studies (COTTON and

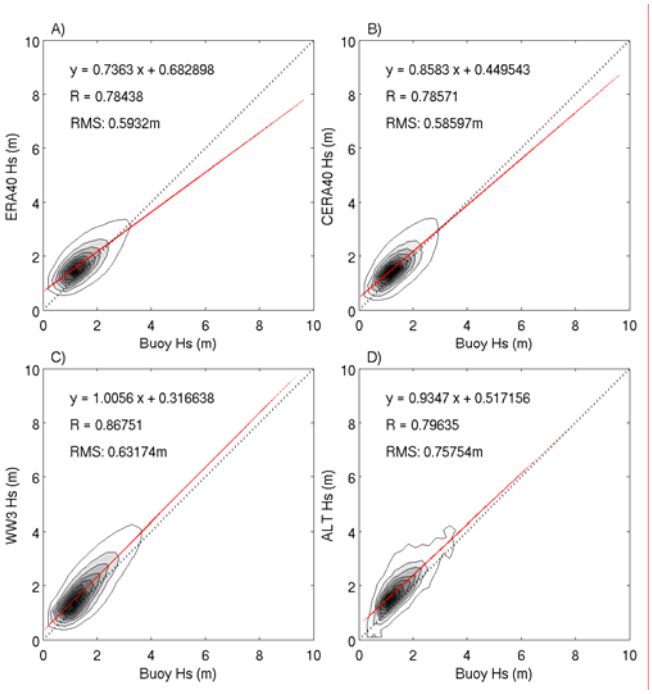

Figure 2. Scatterplots of available wave data against available buoy wave data. a) ERA-40; b) C-ERA-40; c) NWW3; d) altimeter data. The regression line is shown in red. A 1:1 line is dotted black.

CARTER, 1994; CHALLENOR and COTTON, 2002, QUEFFEULOU, 2004)
present corrections to be applied to altimeter-measured H_S values for each mission. Corrections outlined by QUEFFEULOU (2004) provided the best comparison with buoy data and were applied here.

Altimeter wave height data to be compared with buoy-measured wave heights have been selected as those data measured within a 30km radius of a buoy and occur within a six-hour time window centred on a buoy observation. This results in 11962 aligned H_S points for all 30 buoys. In the mid-inner shelf region, where most buoys are located, the 30km radius introduces significant geophysical variance. If a smaller radius is chosen, the number of data available for comparison reduces. 30km was chosen as a compromise between number of data points and minimising geophysical variance. Tests were carried out at a single buoy location (Cape de Couedic, South Australia) to determine the relationship between catchment radius and the regression statistics. Cape de Couedic was chosen as wave properties were considered to vary minimally with distance on exposed coast. Table 1 indicates that smaller radius values result in greater correlation and reduced RMS errors.

Figure 2D shows a scatter plot of altimeter-measured and waverider buoy measured H_S from the 16 'exposed' buoys, and associated regression statistics displayed. Note that when data from all 30 buoys are used for comparison, regression statistics remain relatively unchanged, suggesting that altimeters are well suited to measuring wave heights at all buoy sites.

Table 1. Variation of regression statistics with changing radius of altimeter data catchment (D) at Cape de Couedic. N is number of points; m is slope of regression line; c is regression intercept; R is Pearson's correlation coefficient; and RMSE is the Root Mean Square Error.

D (km)	N	M	c	R	RMSE (m)
10	169	0.996	0.185	0.9481	0.3263
20	518	1.017	0.122	0.9216	0.4067
30	1029	0.941	0.344	0.8584	0.5447

INTERCOMPARISON OF AUSTRALIAN WAVE CLIMATE FOR COMMON PERIOD

A five-year period exists from March, 1997 to February, 2002 for which data is available from ERA-40, C-ERA-40, NWW3, and altimeter datasets. Fourteen Australian waverider buoys also span this period, ten of which occur on 'model grid resolved' coastline.

Five-year Mean Significant Wave Heights

The five-year mean H_S from four spatial datasets was determined (Figure 3). ERA-40 values underestimate those computed from other datasets by approximately 0.5m in the Southern Ocean (south of 25°S), qualitatively consistent with CAIRES and STERL (2005), who state that ERA-40 consistently underestimates large wave events, particularly in the Southern Ocean. The altimeter dataset exhibits the largest difference in comparison with the buoy data when comparing five-year means. It was shown above that altimeter H_S displays good agreement when the radius about the buoy is chosen to be small. Therefore, the large difference is expected to result from the coarsely-gridded data. The C-ERA-40 data has the smallest RMS error (0.30 m) when comparing five-year means with the ten chosen buoys.

The map of mean H_S from all datasets indicates largest waves (in excess of 4.5m) to the south-west of the Australian continent. The sheltering effect of the Australian landmass from the westerly swell is observed, with smaller H_S on the east coast than the west coast at the same latitude. A tongue of increased H_S is observed extending into the Tasman Sea between the NSW coast and New Zealand. These increased wave heights are likely due to the directional spread of Southern Ocean swell propagating into the Tasman Sea from the Southern Ocean. Mean H_S in the north of the country are significantly less than those along the Southern margin. Mean H_S are typically less than 1m in the Arafura Sea and do not exceed 2m at any point along the Queensland coast.

Mean Annual Cycle

The mean annual cycle from all datasets was determined by calculating the monthly means over the five-year period (Figure 4). Mean significant wave heights are significantly greater in the west

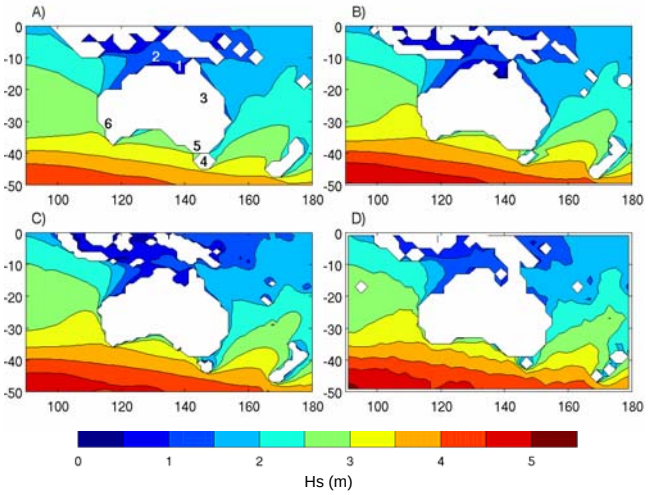

Figure 3. Maps of five-year mean significant wave height (m) for the Australian region. a) ERA-40 dataset, RMS error from mean calculated at 10 buoy locations is 0.44m; b) C-ERA-40 dataset, RMS error is 0.30m; c) NWW3 dataset, RMS error is 0.44m; d) altimeter dataset, RMS error is 0.52m. Altimeter measured wave height has been gridded on a 2° x 2° latitude-longitude grid. Numbered in a) are locations mentioned in the text: 1) Gulf of Carpentaria; 2) Arafura Sea; 3) Queensland coast; 4) Tasmania; 5) Victoria; and 6) WA.

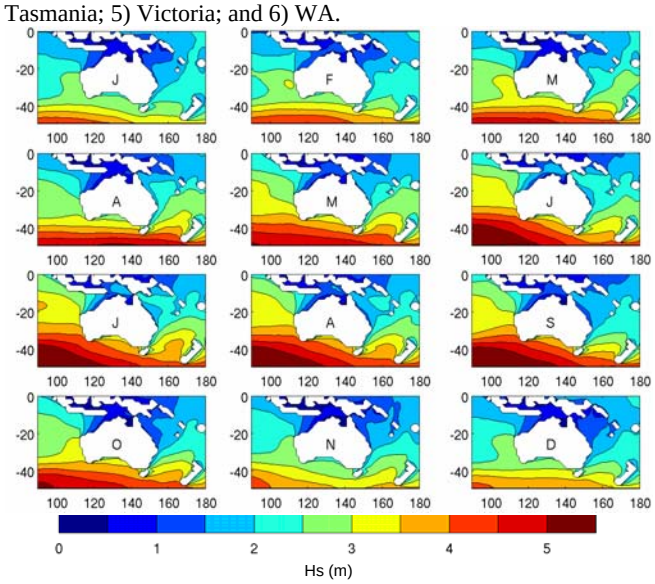

Figure 4. Mean annual cycle of significant wave height (m) (monthly means) as computed from the C-ERA-40 dataset over the five-year common data period (02/1997-01/2002).

and south-west of the region during the months June-September. These increased Southern Ocean waves are associated with the northward shift of the westerlies during the winter months. Wave heights are also observed to increase along the Queensland coast and in the Arafura Sea during the months of June and July. These occur at the peak of the south-easterly trade wind season, thus increasing fetch in these regions. During the north-westerly monsoon season (Dec-March), H_S are less than 1m throughout this region.

Datasets were inter-compared over the five-year period. C-ERA-40 and NWW3 display best agreement between mean annual cycles of Hs, with mean percentage error less than 10% over the entire region. Maximum differences occur between C-ERA40 and ERA-40, and C-ERA-40 and the altimeter measured waves. C-ERA-40 is consistently 10% greater than altimeter data over the whole Australian region and 15-20% greater than ERA-40 in the Southern Australian region. The amplitude of the ERA-40 mean annual cycle overestimates altimeter-measured Hs in the tropics by approximately 10% and underestimates by approximately 5% in the southern region. ERA-40 H_S are approximately 0.5m low in the south-west Australian region during the winter months. During summer months, bias is reduced to approximately 0.1m.

Inter-annual variability

The sample standard deviation (an estimate of the inter-annual variability of significant wave height) was determined and normalised by the mean H_S. The normalised standard deviation of H_S is mapped for C-ERA-40 data in Figure 5. Absolute inter-annual variability (not shown) is greatest in the region south of Australia (influencing the south-west coasts of Victoria and Tasmania) and South Australia's south-east coast, particularly during May and September. During March, significant variability is observed off the Queensland coast associated with the passage of a cyclone during one of the sample years.

Variability of 5-10% of the mean H_S is typical throughout the Australian region (Figure 5) and is greatest in the Gulf of Carpentaria, the Arafura Sea and off the Queensland coast during the monsoon and months of cyclone generation with variability being approximately 35% of the mean.

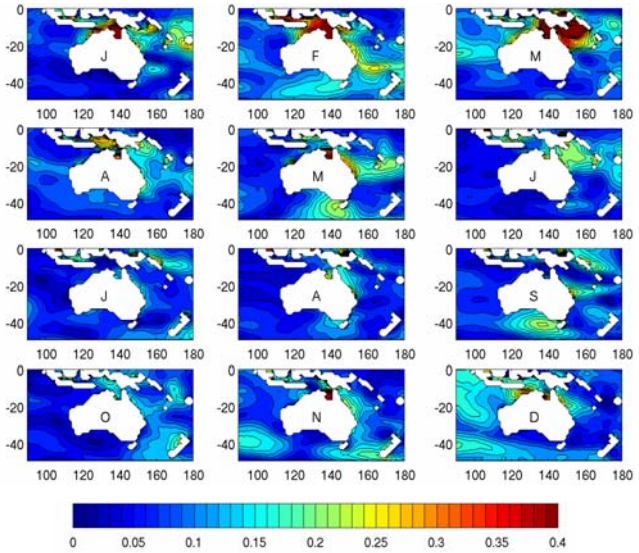

Figure 5. The sample standard deviation of monthly mean significant wave heights, normalised by the mean significant wave height (dimensionless).

PATTERNS OF VARIABILITY IN THE AUSTRALIAN WAVE CLIMATE

Variability and unpredictability is expected at the scale of individual atmospheric cyclones; however, high interannual variability in the monthly statistics suggests more coherent patterns are involved.

Having identified that the C-ERA-40 dataset provides reasonable estimates of the significant wave heights in the Australian region, the full 45-yr record is further investigated. A similar analysis of other datasets is to be undertaken at a later date.

Six sub-datasets were created: 1) the monthly anomaly wave heights (the monthly mean data for each month in the 45-yr record, with the corresponding mean value from the mean annual

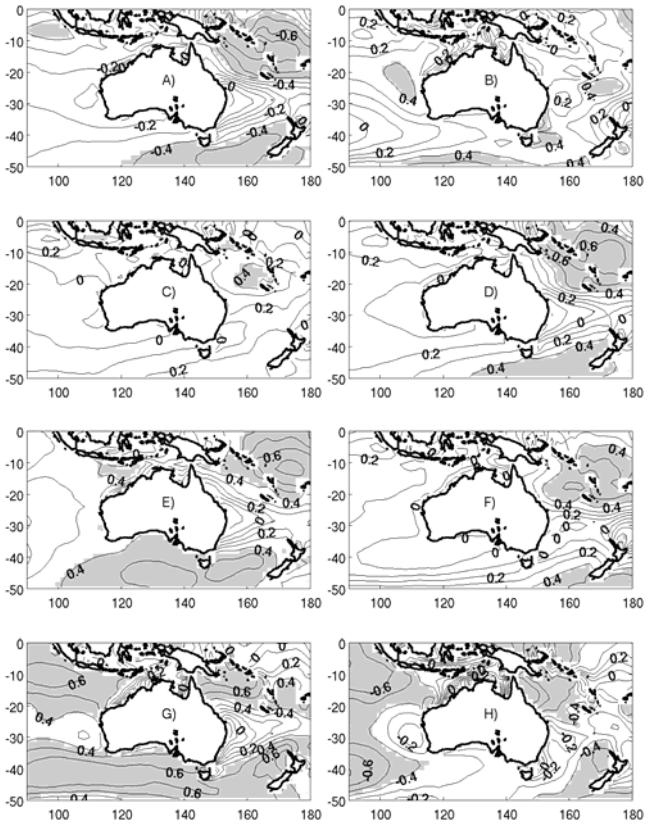

Figure 6. Contour map of correlation coefficient resulting from linear regression of annual mean significant wave height and climate indices. a) SOI; b) SAMI; c) IOD; d) Nino-3 SST; e) PDO; f) Australian region annual mean pressure anomaly; g) Mean zonal wind speed anomaly in Australian region south of 23.5°S; h) Mean zonal wind speed anomaly in Australian region north of 23.5°S. Shaded grey indicates the correlation is significant at the 1% level.

cycle removed); 2) annual mean wave heights; 3-6) seasonal means (DJF, MAM, JJA and SON, respectively).

The gridded mean significant wave heights of the six sub-datasets have been regressed against a number of climatological indices to determine what drives Australia's wave climate. The indices tested to date include: 1) The Southern Oscillation Index (SOI); 2) The Southern Annual Mode Index (SAMI); 3) The Indian Ocean Dipole (IOD) Index; 4) The Nino-4 SST Index; 5) The Nino-3 SST Index; 6) The Pacific Decadal Oscillation (PDO); 7) The mean sea level pressure monthly anomaly for the Australian region, calculated by subtracting the corresponding mean value within the dataset of the corresponding calendar month; 8) The mean zonal wind anomaly in the Australian region south of 23.5°S; 9) The mean zonal wind anomaly in the Australian region north of 23.5°S; and 10) the number of cyclones per year in the Australian region. Figure 6 shows contour maps of the correlation coefficient resulting from linear regression analysis of the gridded annual mean H_S against each climatological index. Correlation to number of tropical cyclones, indicating a small area of significant correlation centred at 15°S, 160°E, is not shown. The strongest relationships are for regression against the mean zonal wind speed in the Australian region south of 23.5°S. Significant correlation against the SOI index (and the related Nino-3 and Nino-4 indices; Nino-4 is not shown) is also observed to the east of the Australian continent. Correlation to the SOI is strongest during winter and spring months in this region (not shown). A strong relationship between El-Nino and waves in the Tasman and

Coral Seas has been previously recognised by LAING (2000), ALLEN and CALLAGHAN (2000) and TREMBANIS *et al*. (2001). Significant correlation to the PDO is observed in the region south of the Australian continent. This is the result of an observed minimum in significant wave height in the C-ERA-40 H_S data in September, 1975 and an apparent change in the level of the H_S time series before and after this minimum. STERL and CAIRES (2005) suggest that although the 09/75 minimum may be a real feature, the change in level is most likely due to assimilation of satellite data from 1979 onwards. The change in level corresponds in time with a change in phase of the PDO.

CONCLUSIONS

Satellite altimeter-derived significant wave heights, wave-rider buoy data and global wave model output from ERA-40, C-ERA-40 and NWW3 were obtained to describe Australia's wave climate. Inter-comparison of available Hs data indicates good agreement. Comparisons to ERA-40 data indicate ERA-40 underestimates winter wave heights South of Australia.

The long-term mean and mean annual cycle of significant wave heights in the Australian region have been determined, outlining the importance of trade and monsoon winds in the north and the location of the band of westerly winds in the south.

Absolute interannual variability of significant wave heights is greatest along the western Tasmanian coast; however, as a fraction of the mean wave height, variability is as much as 40% in cyclone-affected regions. The interannual variability has been shown to be dominated by variability in the zonal wind velocities, particularly in the south of the region. Variability in the Tasman and Coral Seas is correlated to the Southern Oscillation Index. The influence of the Interdecadal Pacific Oscillation on Australia's wave climate remains unresolved due to unreliability of ERA-40 wave model output at the time of the key PDO phase shift in the late 1970s.

Investigation into determining which climate mechanisms control variability of Australia's wave climate is continuing. Further investigation of the remaining datasets and the associated variability of wave directions and of wave height extremes are still to be carried out.

LITERATURE CITED

AGO, 2006. Assessing and mapping Australia's coastal vulnerability to climate change: Expert Technical workshop. 13-14 Dec, 2005. Department of Environment & Heritage, Australian Greenhouse Office. Canberra. 31pp.

ALLEN M.A. AND CALLAGHAN J. 2000, *Extreme wave conditions for the South East Queensland coastal region.* Technical Report 32, Environmental Protection Agency, Brisbane.

CAIRES, S. AND STERL, A., 2005. A new non-parametric method to correct model data: Application to Significant Wave Height from the ERA-40 Re-Analysis. *Journal of Atmospheric and Oceanic Technology*, 22, 443-459.

CHALLENOR, P.G. AND COTTON, P.D., 2002. The joint calibration of altimeter and in-situ wave heights, in *Advances in the Applications of Marine Climatology – The dynamic part of the WMO guide to the applications of marine climatology, WMO/TD-No. 1081 JCOMM Tech. Rep. No. 13,* World Meteorol. Organ., Geneva.

COTTON, P.D. AND CARTER, D.J.T., 1994. Cross-calibration of TOPEX, ERS-1, and Geosat wave heights. *J. Geophys. Res.*, 99**,** 25025-25033, Correction, 1995. *J. Geophys. Res.*, 100, 7095

ECMWF, 2006. European Centre for Medium Range Weather Forecasting. Website: http://www.ecmwf.int/era-40. Accessed 8-Oct-2006.

GOODWIN, I.D., 2005. A mid-shelf, mean wave direction climatology for south-eastern Australia and its relationship to the El Niño - Southern Oscillation since 1878 A.D. *International Journal of Climatology*., 25(13), 1715-1729.

KOMEN, G.J.; CAVALERI, L; DONELAN, M.; HASSELMANN, K.; HASSELMANN, K.; AND JAENSEN, P.A.E.M., 1994. *Dynamics and modelling of ocean waves.* Cambridge University Press, 532 pp.

KULMAR, M.A. 2000. Wave direction distributions off Sydney, New South Wales. In *Proceedings, 12th Australasian Coastal and Ocean Engineering Conference*, Melbourne; 175-181.

LAING, A.K., 2000. New Zealand wave climate from satellite observations. *New Zealand Journal of Marine and Freshwater Research*, 34, 727-744.

LIONELLO, P., AND A. SANNA, 2005. Mediterranean wave climate variability and its links with NAO and Indian Monsoon. *Climate Dynamics*, 25(6), 611-623.

QUEFFEULOU, P., 2004. Long-term validation of wave height measurements from altimeters. *Marine Geodesy*, 27, 495-510.

SCHRAMA, E.; SCHARROO, R. AND M. NAEIJE, 2000. Radar Altimeter Database System (RADS): Towards a generic multi-satellite altimeter database system, Final Report. *SRON/BCRS publ., USP-2 report 00-11*, 88p.

SHORT, A.D. AND TRENEMAN, N.L., 1992. Wave climate of the Sydney region, an energetic and highly variable ocean wave regime. *Aust. J. Mar. Freshwater Res.*, 43, 765-791.

STERL, A. AND CAIRES, S., 2005. Climatology, variability and extrema of ocean waves: The web-based KNMI/ERA-40 wave atlas. *International Journal of Climatology*, 25, 963-977.

TOLMAN, H. L. 1999. User manual and system documentation of WAVEWATCH-III version 1.18. NOAA / NWS / NCEP / OMB Technical Note 166 , 110 pp.

TREMBANIS, A.C.; SMITH, S.A.W. AND SHORT, A.D., 2001. El-Nini/Southern Oscillation (ENSO), Wave climate, and beach variation – Two case studies from Australia. *GSA Earth Systems Processes Global Meeting 24-28 June 2001, Edinburgh.* Poster.

WALSH, K.J.E.; BETTS, H.; CHURCH, J.; PITTOCK, A.B.; MCINNES, K.L.; JACKETT, D.R. AND MCDOUGALL, T.J., 2004. Using sea level rise projections for urban planning in Australia. *Journal of Coastal Research*, 20(2), 586-598.

WOOLF, P.K.; CHALLENOR, P.G. AND COTTON, P.D., 2002. Variability and predictability of the North Atlantic wave climate. *Journal of Geophysical Research*, 107(C10), doi:10.1029/2001JC001124.

ACKNOWLEDGEMENTS

This paper is a contribution to the CSIRO Climate Change Research Program and the sea-level rise program of the Antarctic Climate and Ecosystems Co-operative Research Centre. Research is supported by funding from the Australian Greenhouse Office, Department of Environment & Heritage and Australian Commonwealth. We thank ECMWF for ERA-40; Andreas Sterl (KNMI) for C-ERA-40; NOAA for NWW3; The Bureau of Meteorology; Manly Hydraulics Laboratory, New South Wales State Government; Environmental Protection Authority (EPA), Queensland State Government; Department of Primary Industries, West Australian State Government; and the Port of Melbourne for buoy data.